

Diffusion-Based Noise Analysis for Molecular Communication in Nanonetworks

Massimiliano Pierobon, *Member, IEEE*, and Ian F. Akyildiz, *Fellow, IEEE*

Abstract—Molecular communication (MC) is a promising bio-inspired paradigm, in which molecules are used to encode, transmit and receive information at the nanoscale. Very limited research has addressed the problem of modeling and analyzing the MC in nanonetworks. One of the main challenges in MC is the proper study and characterization of the noise sources. The objective of this paper is the analysis of the noise sources in diffusion-based MC using tools from signal processing, statistics and communication engineering. The reference diffusion-based MC system for this analysis is the physical end-to-end model introduced in a previous work by the same authors. The particle sampling noise and the particle counting noise are analyzed as the most relevant diffusion-based noise sources. The analysis of each noise source results in two types of models, namely, the physical model and the stochastic model. The physical model mathematically expresses the processes underlying the physics of the noise source. The stochastic model captures the noise source behavior through statistical parameters. The physical model results in block schemes, while the stochastic model results in the characterization of the noises using random processes. Simulations are conducted to evaluate the capability of the stochastic model to express the diffusion-based noise sources represented by the physical model.

Index Terms—Molecular communication, molecule counting noise, nanonetworks, nanotechnology, particle diffusion, Poisson noise.

I. INTRODUCTION

NANOTECHNOLOGY is nowadays one of the most promising emerging research fields, enabling devices manufactured in a scale ranging from one to a hundred nanometers. At this scale, a nanomachine is considered to be the most basic structural and functional device, consisting of nanoscale components, and able to perform tasks at the nano-level, such as computing, data storing, sensing or actuation. Nanomachines can be interconnected as a network, or nanonetwork [1], to execute more complex tasks and to expand their range of operation. The characterization of communication mechanisms between

nanomachines, the definition of channel models and the development of architectures and protocols for nanonetworks are new challenges that need to be addressed in the research world.

Molecular communication (MC) is a promising paradigm for communication in nanonetworks. Unlike classical communication techniques, we believe that the integration process of molecular transceivers in nanomachines is more feasible due to their size and natural domain. MC follows a bio-inspired approach, in which molecules are used to encode, transmit and receive information at the nanoscale. Several techniques to propagate information molecules have been proposed so far [2], ranging from molecular motors [3], to bacteria [4] or free diffusion [5]. We focus on the diffusion-based architecture, as it represents the most general and widespread MC architecture found in nature. Pheromonal communication, when pheromones are released into a fluidic medium [6], such as air or water, is an example of diffusion-based architecture. Another example is calcium signaling among cells [7]. Different mathematical models have been formulated for the diffusion of molecules in a fluid. As an example, the theory of turbulent diffusion [8] can be applied to the diffusion of pheromones, while the theory of electro-diffusion [9] is applicable to the diffusion of calcium ions in calcium signaling. The most general model of molecular diffusion in fluids, which underlies all the other models, is based on the Fick's diffusion theory [10], [11]. In this paper, we consider only Fick's diffusion in order to maintain the maximum possible generality for our diffusion-based MC system. Further specifications of the system for the pheromonal communication case or the calcium signaling case stem from the general case treated in this work.

Up to date, very limited research has addressed the problem of the analytical modeling of diffusion-based MC from an information theoretical point of view. While in [12] some open questions about nanoscale information theory are outlined, concrete mathematical solutions for specific diffusion-based MC architectures are not provided. Two main different diffusion-based MC architectures have been studied by the research community under an information theoretical point of view, on the basis on how information is encoded in the diffusing molecules. In [13], the information is encoded in the time of release of each molecule in the diffusion channel, while in [14]–[17], the information is encoded into variations in the concentration of molecules in the space. The first type of architecture is theoretically analyzed in [13], where the authors focused on the mathematical modeling of the diffusion channel as a probabilistic contribution in the time of arrival of molecules at the receiver. The model of this system is focused on the diffusion channel, while the transmitter is an ideal emitter of one or more molecules at precise time instants, and the receiver ideally computes the molecule time of arrival at its location. Moreover, a drift velocity is added on top of the diffusion process. The results of simulations from

Manuscript received July 06, 2010; revised October 11, 2010 and January 13, 2011; accepted January 14, 2011. Date of publication February 14, 2011; date of current version May 18, 2011. The associate editor coordinating the review of this manuscript and approving it for publication was Dr. Z. Jane Wang. This material is based upon work supported by the U.S. National Science Foundation under Grant CNS-0910663.

M. Pierobon is with the Broadband Wireless Networking Laboratory, School of Electrical and Computer Engineering, Georgia Institute of Technology, Atlanta, GA 30332 USA (e-mail: maxp@ece.gatech.edu).

I. F. Akyildiz is with the Broadband Wireless Networking Laboratory, School of Electrical and Computer Engineering, Georgia Institute of Technology, Atlanta, GA 30332 USA, and also with the N3Cat (NaNoNetworking Center in Catalunya), Universitat Politècnica de Catalunya (UPC), 08034 Barcelona, Catalunya, Spain (e-mail: ian@ece.gatech.edu).

Color versions of one or more of the figures in this paper are available online at <http://ieeexplore.ieee.org>.

Digital Object Identifier 10.1109/TSP.2011.2114656

[13] in terms of achievable information rate show that, due to the high uncertainty in the propagation time, this architecture is characterized by very low capacity. The work in [14] and [15] is focused on developing an MC receiver model based on molecule concentration encoding, while the transmitter and the diffusion-based propagation theory are not taken into account. In [16], a simplified receiver model that receives one molecule at a time is coupled with a diffusion-based channel model, while the transmitter is an ideal molecule rate emitter. In [17], a physical model of the diffusion-based MC is developed in terms of end-to-end information delivery at the nanoscale and models are provided for the transmitter, the channel and the receiver. A third possible diffusion-based MC architecture is proposed and analyzed in [18], where information is encoded in each single molecule and only the diffusion channel part is modeled, together with other types of channels. As a consequence, the information carried by a certain molecule is received only if that molecule reaches the receiver location.

The proper study and characterization of the noise is one of the main challenges in the information theoretical analysis of diffusion-based MC. Most of the works from the literature do not provide stochastic models for the noise sources in terms of random processes. The results of these works are expressed in terms of system capacity computed on numerical results from large sets of simulations. A non-Gaussian noise is observed through numerical results from simulations of the system proposed in [16], even if it is not analytically modeled with a closed-form expression of a random process. Also in [18], the noise effects on the diffusion-based MC are resulting only from simulations and there is no analytical model of diffusion-based noise and no stochastic study of its underlying physical phenomena. In [19], the noise analysis stems from a formulation of the ligand-receptor reaction kinetics at the receiver side, without accounting for diffusion. A numerical evaluation of the system capacity is here provided in terms of probability of having erroneous digital reception, but only under the assumption of a binary squared pulse code modulation signal. In [13], a mathematical equation for finding the system capacity is provided and it is evaluated with numerical methods.

In this paper, we aim at the analysis of the most relevant diffusion-based noise sources affecting MC. We use tools from signal processing, statistics and communication engineering, with the aim to obtain stochastic models of the sources in terms of random processes. The reference diffusion-based MC system for this analysis is the physical end-to-end model introduced in [17].

Contributions from the biochemistry literature provide descriptions of some physical processes underlying the noise sources in diffusion-based MC systems. Seminal works in biochemistry, such as [20], analyzed how free space diffusion of molecules impairs the proper measurement of the molecule concentration. A more recent contribution to the physical analysis of molecule diffusion and reception in biochemical signaling can be found in [21]. However, these contributions tend to focus on the explanation of natural phenomena and do not provide suitable models for MC engineering. The work in [22] stems, on the contrary, from the simulation of a biological signal transduction mechanism and its associated noise using tools from communication engineering. However, the analysis

of the system is limited to a numerical evaluation of the simulation results using communication engineering parameters [e.g., the signal-to-noise ratio (SNR)]. No stochastic models are provided in [22] for the noise sources, but the results are coming from numerical simulations. In [23], the authors develop only a preliminary information theoretic model applied to the study of intracellular communication with the diffusion of calcium ions.

The noise sources considered in this paper are modeled in a twofold fashion: the physical model provides a mathematical analysis of the physical processes which generate the noise, while the stochastic model aims at capturing those physical processes through statistical parameters. The physical model contains all the physical variables which contribute to the generation of the noise. The stochastic model summarizes the noise generation using random processes and their associated parameters. While the physical model provides a means to simulate the generation of noise in MC, the random nature of the diffusion processes does not allow for a deterministic knowledge of the noise signal. Noise impairments on MC can be studied only statistically through the parameters of the stochastic model. Sets of noise data realizations are generated through simulation of the physical model. The sets of noise data are then used to test the stochastic model ability to capture the behavior of the physical processes which generate the noise.

The remainder of the paper is organized as follows. In Section II, some assumptions for the proposed noise analysis are introduced, and the diffusion-based noise sources are briefly defined with reference to the end-to-end model from [17]. The first noise source, namely, the particle sampling noise, is analyzed in Section III, whereas the second noise source, namely, the particle counting noise, is treated in Section IV. The physical models for the two noise sources are introduced in Sections III-A and IV-A, while the stochastic models are outlined in Sections III-B and IV-B, respectively. Simulations are provided in Section V for each noise source with the objective to test the stochastic model ability to capture the behavior of the physical models. Finally, in Section VI, we conclude the paper and present some future open research problems.

II. THE DIFFUSION-BASED NOISE IN THE END-TO-END MODEL

The end-to-end (including channel) model from [17] describes the diffusion-based MC in terms of transmission, propagation and reception of particles, as sketched in Fig. 1. The three-dimensional space S is here indexed through the Cartesian axes X , Y , and Z . The transmitter is placed at the axes origin. The emission process modulates the particle concentration rate at the transmitter according to an input signal. The modulation is achieved through the release/capture of particles into/from the emission gaps. The modulated particle concentration rate is the output of the transmitter and the input of the propagation. The propagation relies on the diffusion process of the particles in the space S to output the particle concentration at the receiver. The receiver senses the variations in the particle concentration at its location as input and it recovers the output signal. The reception process generates the output signal by means of chemical receptors. A mathematical analysis of the communication channel of Fig. 1 is provided in [17] by comparing the input and the output signals. The normalized gain and delay between inputs and outputs are

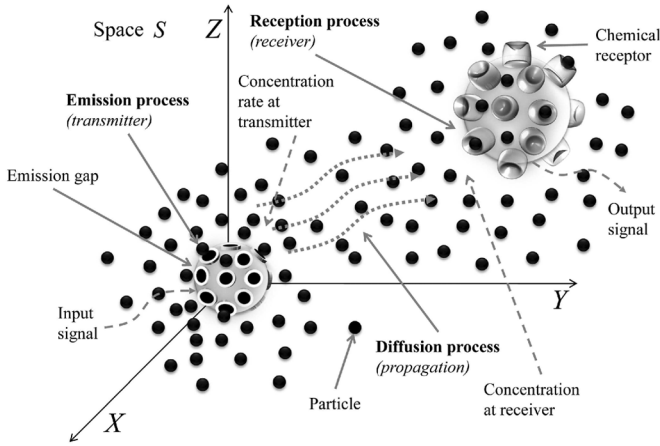


Fig. 1. Graphical representation of the end-to-end model.

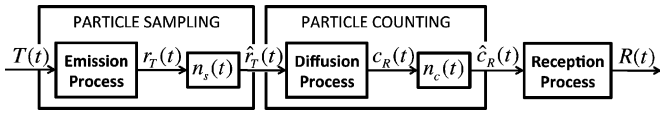


Fig. 2. Block scheme of the end-to-end model and the diffusion-based noise sources.

computed as functions of the frequency and the transmission range for the three underlying physical processes, namely, the particle emission, diffusion and reception, as well as for the overall end-to-end model. However, the analysis from [17] does not account for diffusion-based noise effects on the information signal as it propagates through the end-to-end model. In this paper, we complete the model introduced in [17] by providing an analysis of the possible diffusion-based noise sources.

The analysis of the diffusion-based noise sources stems from the assumptions defined for the end-to-end model in [17]:

- All the processes take place inside the space S , with reference to Fig. 1, which contains a fluidic medium and it has infinite extent in all three dimensions.
- A particle is an indivisible object that can be released into, or collected from, the space S .
- When a particle is not being released or collected, it is subject to the diffusion process in the fluidic medium contained in the space S .
- The shape, size and mass of a particle are considered negligible.

Two type of noises are identified and studied in this paper, namely, the particle sampling noise and the particle counting noise. The particle sampling noise and the particle counting noise are analyzed as the most relevant diffusion-based noise sources affecting the physical end-to-end model in Sections III and IV, respectively. In the following, we define each noise source with reference to the block scheme in Fig. 2.

The “PARTICLE SAMPLING” is related to the **Emission Process** at the transmitter. During the emission process, particles are emitted from the particle transmitter according to the input signal $T(t)$, which modulates the particle concentration rate $r_T(t)$ at the transmitter location:

$$T(t) \rightarrow r_T(t). \quad (1)$$

According to the transmitter model in [17], the modulation of the particle concentration rate does not follow any specific digital modulation scheme. The signal $T(t)$ can be in general any continuous function of the time t and the modulated particle concentration rate $r_T(t)$, output of the transmitter, is a function of $T(t)$. The particle sampling noise is expressed as $n_s(t)$. The effect of $n_s(t)$ is an unwanted perturbation on the output of the emission process $r_T(t)$, which results in $\hat{r}_T(t)$:

$$r_T(t) \rightarrow \hat{r}_T(t). \quad (2)$$

The particle sampling noise is generated by the “PARTICLE SAMPLING,” which occurs when the particle concentration rate $\hat{r}_T(t)$ is being modulated through the emission of the particles. The noise effects arise from the discreteness of the particles that compose the particle concentration rate $\hat{r}_T(t)$. The particle concentration rate $r_T(t)$ in output from the emission process is caused by a particle flux between the transmitter and the external space. Given the discreteness of the particles, the particle concentration rate $r_T(t)$ is sampled by the particles themselves, resulting in the particle concentration rate $\hat{r}_T(t)$. Further details on the analysis for this type of noise are provided in Section III.

The “PARTICLE COUNTING” is related to the signal propagation due to the **Diffusion Process**. The signal contained in the particle concentration rate $\hat{r}_T(t)$ propagates due to the particle diffusion from the transmitter location to the receiver location. The particle concentration value $c_R(t)$, a measure of the particle concentration at the receiver location, is the output of the diffusion process:

$$\hat{r}_T(t) \rightarrow c_R(t). \quad (3)$$

According to the signal propagation model in [17], the modulated particle concentration rate $\hat{r}_T(t)$ creates differences in particle concentration across the space S . These differences cause a nonhomogeneous particle concentration inside the space S which, due to the particle diffusion, causes variations in the particle concentration $c_R(t)$ at the receiver location. The particle counting noise is expressed as $n_c(t)$. The effect of $n_c(t)$ is an unwanted perturbation on the output of the diffusion process $c_R(t)$, which results in $\hat{c}_R(t)$:

$$c_R(t) \rightarrow \hat{c}_R(t). \quad (4)$$

The particle counting noise occurs when the particle concentration value is being measured at the receiver location (“PARTICLE COUNTING”), and it is due to the randomness in the movement and to the discreteness of the particles. The particle concentration $c_R(t)$ at the receiver location is computed by counting the number of particles present in the reception space. Fluctuations and imprecisions in counting the particles impair the proper computation of the concentration $c_R(t)$. The actual computed concentration $\hat{c}_R(t)$ differs from $c_R(t)$. The analysis for this type of noise is provided in Section IV.

During the **Reception Process**, the particle concentration $\hat{c}_R(t)$ at the receiver location is sensed by means of chemical receptors and an output signal $R(t)$ is generated accordingly:

$$\hat{c}_R(t) \rightarrow R(t). \quad (5)$$

According to the analysis presented in this paper, the particle reception process at the receiver is not associated to diffusion-based noise sources. Other types of physical phenomena, which stem from the ligand-receptor kinetics of the chemical receptors, contribute as noise at the receiver. Due to the complexity of these phenomena and to their heterogeneity with respect to the present work, a thorough analysis of the noise sources in the reception process will be presented in a separate future work.

The analysis of the noise sources results both in *physical models* and *stochastic models*. With the former we aim at the mathematical expression of the physical processes underlying the noise sources (Sections III-A and IV-A), while with the latter we model the noise source behaviors through the use of statistical parameters (Sections III-B and IV-B).

The physical models are expressed through the block schemes in Figs. 5 and 10, which expand in detail the blocks $n_s(t)$ and $n_c(t)$ from Fig. 2, respectively. The particle sampling noise physical model is further detailed through (9), (10), (12), (13), (15), and (16), while the particle sampling noise physical model is detailed in (34), (35), (37), (38), (39), (40), (41), and (42).

The stochastic models are analyzed in terms of random processes, such as in (22) and (49), and their effects on the end-to-end model are expressed in terms of root mean square (RMS) perturbation $\tilde{n}_X(t)$ of the noise on the signal, as in (31) and (65). The RMS of the perturbation $\text{RMS}(\tilde{n}_X(t))$ on the signal $s(t)$ (which is $r_T(t)$ or $c_R(t)$, respectively) corresponds to the square root of the average of the squared noise process $\tilde{n}_X^2(t)$:

$$\text{RMS}(\tilde{n}_X(t)) = \sqrt{\langle \tilde{n}_X^2(t) \rangle} \quad (6)$$

where X corresponds to s or c , respectively, and $\langle \cdot \rangle$ denotes the ensemble average operator. The stochastic noise modeling for the aforementioned noise sources is therefore focused on the proper determination of the statistical parameters of their perturbations in relation to the processes expressed by the physical models.

III. THE PARTICLE SAMPLING NOISE

A. The Physical Model

The particle sampling noise affects the physical end-to-end model from [17] at the transmitter. When a signal $T(t)$ has to be delivered through the physical end-to-end model, the transmitter modulates the particle concentration rate $r_T(t)$ at the transmitter location according to the value of $T(t)$ itself. The modulation of the particle concentration rate is achieved by means of the particle emission process, sketched in Fig. 3, which is based on the following assumptions:

- The transmitter has a *spherical boundary* that divides the space in proximity of the transmitter into two areas: the inner area and the outer area.
- The inner concentration $c_T^{\text{in}}(t)$ is the concentration of particles lying in the inner area, whereas the outer concentration $c_T(t)$ is the concentration of particles lying in the outer area.
- The inner area and the outer area are spatially connected by means of *emission gaps*. An emission gap is an opening in the spherical boundary which allows particles to move through due to their diffusion. The size of an emission gap allows only one particle to pass through at each time in-

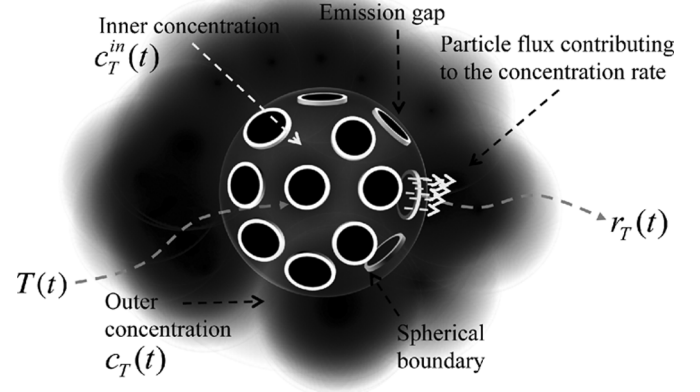


Fig. 3. Graphical sketch of the emission process.

stant. Whenever a particle is traversing the emission gap, its movement has only components along the radius of the spherical boundary. As a consequence, the movement of a particle through the emission gap can only be outward (from the inner area to the outer area) or inward (from the outer area to the inner area). The emission gaps are many and homogeneously distributed on the surface of the spherical boundary. The present noise analysis does not depend on their precise number. We believe it will be important to discuss the impact of the number of emission gaps on the end-to-end model in our future work.

- Whenever there is a difference between the inner concentration $c_T^{\text{in}}(t)$ and the outer concentration $c_T(t)$, a movement of particles is stimulated between the inner area and the outer area through the emission gaps.
- The movement of particles between the inner area and the outer area causes a variation in the outer concentration, whose first time derivative is the particle concentration rate at the transmitter location $r_T(t)$.
- Particles can be created/destroyed in the inner area in order to reach a desired inner concentration $c_T^{\text{in}}(t)$, with reference to the model of the particle emission process from [17]. The creation/destruction of particles in the inner area is supposed to be ideally perfect and instantaneous. As a consequence, we do not account for the randomness that can derive from the creation/destruction of particles. We believe that this is a reasonable approximation that allows us to analyze the noise contributions coming only from the emission process. Further analysis can be conducted by specifying the processes involved in the creation/destruction of particles. As an example, the creation/destruction of particles could be realized through a cascade of chemical reactions or by the emptying/filling of particle reservoirs located in the inner area.
- The transmitter is supposed to be able to adjust the inner concentration $c_T^{\text{in}}(t)$ in order to obtain a particle concentration rate $r_T(t)$ proportional to the signal $T(t)$ (modulation of $r_T(t)$ according to $T(t)$).

Those assumptions are inspired by biochemistry principles related to the living cells and to the mechanisms in cell biosignaling [24]. According to this, the spherical boundary is a simplification of the cell plasma membrane, which separates the

interior of a cell from the outside environment. The emission gaps are inspired by the channels that permit the selective passage of molecules through the plasma membrane of a cell. As an example, the gated ion channels in the plasma membrane are openings that allow the passage of specific ion molecules between the interior of a cell and the outside environment and, amongst others, they serve for cell-to-cell communication purposes. As stated in [24], those ion molecules, while traversing the gated ion channels, are driven by a force that is a sum of two terms. The first term of the force is a function of the difference between the inside and the outside concentration of the same molecules and it depends on the diffusion. The second term of the force is a function of an electrical potential and it is related to the electrostatic charge carried by the ion molecules. Since, according to our assumption, the particles in our system do not carry any electrostatic charge, when they traverse an emission gap they are driven only by the first term of the force. For this, the difference in the concentration of particles between the inner area and the outer area stimulates the driving force that permits their movement through the emission gaps either outward or inward, as explained above.

The model of the emission process provided in [17] does not take into account the discrete nature of the particles when there is a flux between the inner area and the outer area of the spherical boundary. As a consequence, the relation between the input signal $T(t)$ and the resulting particle concentration rate $r_T(t)$ is a continuous function:

$$r_T(t) = f_e(T(t)) \quad (7)$$

where f_e expresses the Emission Process block shown in Fig. 2. We have the additional following assumption for the particle emission process:

- The particle flux between the inner area and the outer area of the spherical boundary is composed of discrete particles. As a result, the relation between the input signal $T(t)$ and the resulting particle concentration rate, denoted by $\hat{r}_T(t)$, is no longer a continuous function. The overall process that takes the input signal $T(t)$ as input and returns $\hat{r}_T(t)$ as output is called “PARTICLE SAMPLING” and it is graphically sketched in Fig. 4. The “PARTICLE SAMPLING” is composed of the Emission Process block and the particle sampling noise block $n_s(t)$, as shown in Fig. 2. During the “PARTICLE SAMPLING,” single particles flowing between the inner area and the outer area contribute to the concentration rate $\hat{r}_T(t)$ with a value k_n at discrete time instants $t_n = t_1, t_2, \dots$. These discrete time instants are not equally spaced, due to the random nature of the particle movements between the inner area and the outer area. As a consequence, the resulting particle concentration rate $\hat{r}_T(t)$ is nonuniformly sampled at randomly spaced time instants t_n , where it assumes values equal to k_n , and it is zero for any other time instant:

$$\hat{r}_T(t) = \sum_{n \in \mathbb{N}} \frac{k_n}{t_n - t_{n-1}} \delta(t - t_n) \quad (8)$$

where $\delta(\cdot)$ is a Dirac delta function. According to the Nyquist theorem [25], since the time instants t_n are randomly spaced, the continuous particle concentration rate $r_T(t)$ can be reconstructed from the nonuniformly sampled particle concentration rate $\hat{r}_T(t)$ if the bandwidth of $r_T(t)$ is limited up to frequency

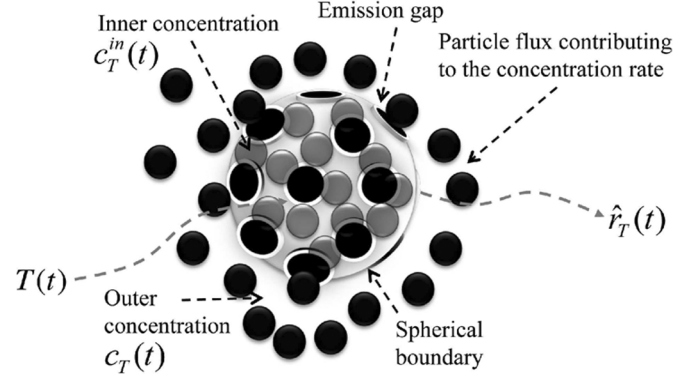


Fig. 4. Graphical sketch of the “PARTICLE SAMPLING”: Emission process and particle sampling noise contribution.

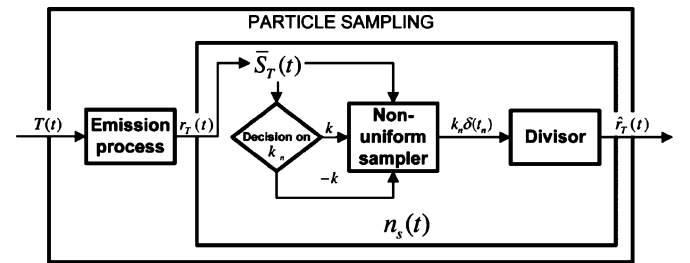


Fig. 5. Block scheme of the particle sampling noise physical model when $t_{n-1} < t < t_{n+1}$.

$1/(2\langle t_n - t_{n-1} \rangle)$, where $\langle t_n - t_{n-1} \rangle$ is the average interval between two consecutive samples of $\hat{r}_T(t)$. As a consequence, given a fixed bandwidth for the system, the degradation caused by the particle sampling noise on the particle concentration rate, output from the transmitter depends on the average rate of the events of single particles flowing between the inner area and the outer area. This event rate corresponds to the particle concentration rate $r_T(t)$ and the system bandwidth depends on the parameters defined in [17]. This result is confirmed through the stochastic model of the particle sampling noise, outlined in Section III-B.

The “PARTICLE SAMPLING” physical model is represented through the block scheme shown in Fig. 5. The signal $T(t)$ is the input of the Emission Process block, whose output is the particle concentration rate $r_T(t)$. The physical model of the particle sampling noise $n_s(t)$ takes as input the particle concentration rate $r_T(t)$ that the emission process would produce in output in the absence of noise. The particle sampling noise $n_s(t)$ is composed of a decision block and a nonuniform sampler, which have as input the transmitter kinetic state $\bar{S}_T(t)$, and a divisor. The output of the particle sampling noise $n_s(t)$ is the particle concentration rate affected by noise, namely, $\hat{r}_T(t)$.

The **transmitter kinetic state** $\bar{S}_T(t)$, as shown in Fig. 6, is a set composed by the location $\bar{x}_p(t)$ and the net velocity $\bar{v}_p(t)$ of each particle p at time t present in the surrounding of the transmitter spherical boundary

$$\bar{S}_T(t) = \{\bar{x}_p(t), \bar{v}_p(t) | p = 1, \dots, P(t)\} \quad (9)$$

where $P(t)$ is the number of particles in the system and varies as a function of the time t . The net velocity $\bar{v}_p(t)$ is here defined as the nonisotropic component of a particle speed, in contrast

to the Brownian motion in free space which has isotropic components. In order to realistically simulate the transmitter kinetic state $\bar{S}_T(t)$, we consider two different contributions to the particle displacement, namely, the Brownian motion and the time integral of the particle net velocity from time instant t_0 to time instant t . The time instant t_0 corresponds to the beginning of the emission process. The expression of the particle location $\bar{x}_p(t)$ is written as follows:

$$\bar{x}_p(t) = b_x(t)\hat{i} + b_y(t)\hat{j} + b_z(t)\hat{k} + \int_{t'=t_0}^t \bar{v}_p(t')dt' \quad (10)$$

where the Brownian motion components, namely, $b_x(t)$, $b_y(t)$, and $b_z(t)$, are random variables with normal distribution, zero mean value and variance equal to $2D\delta t$, according to the expression of the Wiener process [26]:

$$b_x(t), b_y(t), b_z(t) \sim \mathcal{N}(0, 2D\delta t) \quad (11)$$

along the versors of the Cartesian axes, namely, \hat{i} , \hat{j} , and \hat{k} . D is the diffusion coefficient and δt is the simulation time step and it depends on how the transmitter kinetic state is sampled during the physical model simulation. The smaller is the time step δt , the closer is the simulation to the real physical phenomenon of particle diffusion. The value of the time step δt defines the time resolution with which we model events concerning particles changing their space area. According to the Nyquist theorem [25], if the value of the time step δt is smaller than $1/(2B_{r_T})$, where B_{r_T} is the bandwidth of the particle concentration rate $r_T(t)$, then we can have a perfect simulation of the sampling noise generation as it happens in reality. When the particle is located inside the inner area or the outer area, it is only subject to the Brownian motion. In these cases, the particle speed has only the isotropic components due to the Brownian motion in free space, and its net velocity $\bar{v}_p(t)$ is equal to zero. When the particle is traversing an emission gap, its movement can only be outward in case of positive rate ($r_T(t) > 0$) or inward in case of negative rate ($r_T(t) < 0$) along the radius of the spherical boundary. In order to quantify the particle net velocity $\bar{v}_p(t)$, we consider that the particle concentration rate $r_T(t)$ is given only by the contribution of the particles traversing the emission gaps. Given a particle concentration rate $r_T(t)$, the number of particles traversing the emission gaps in a unit time is given by the transmitter inner concentration $c_T^{\text{in}}(t)$ in case of positive rate ($r_T(t) > 0$) and by the transmitter outer concentration $c_T(t)$ in case of negative rate ($r_T(t) < 0$), multiplied by their average velocity. When they traverse the emission gap, the particle average velocity corresponds to the net velocity $\bar{v}_p(t)$. As a consequence, the particle net velocity $\bar{v}_p(t)$ is proportional to the particle concentration rate $r_T(t)$, divided by the transmitter inner concentration $c_T^{\text{in}}(t)$ in case of positive rate ($r_T(t) > 0$), or divided by the transmitter outer concentration $c_T(t)$ in case of negative rate ($r_T(t) < 0$):

$$\bar{v}_p(t) = \begin{cases} 0, & \text{if } p \text{ in inner or outer} \\ \frac{r_T(t)}{c_T^{\text{in}}(t)\mathbf{1}_{r_T(t)>0} + c_T(t)\mathbf{1}_{r_T(t)<0}}\hat{\gamma}, & \text{if } p \text{ in emission gap} \end{cases} \quad (12)$$

where $\mathbf{1}_{(\text{condition})}$ is equal to 1 when *condition* is true and 0 otherwise. $\hat{\gamma}$ is the versor along the radius of the transmitter spherical boundary.

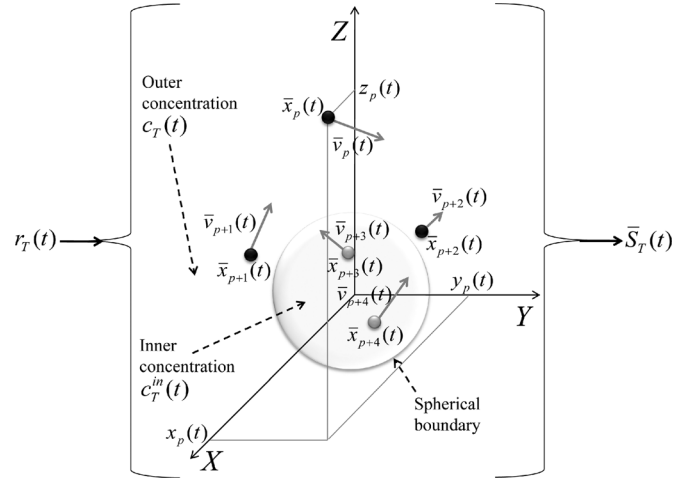


Fig. 6. Graphical sketch of the transmitter kinetic state $\bar{S}_T(t)$ at time t . $\bar{S}_T(t)$ depends on the particle concentration rate $r_T(t)$ in input through the expressions in (9) and (10).

The **decision** block assigns the value of k_n according to the transmitter kinetic state $\bar{S}_T(t)$. k_n is assigned a positive k value or a negative $-k$ value according whether there is an event in the kinetic state $\bar{S}_T(t)$ concerning a particle changing its space area, e.g., from the inner to the outer area, with contribution k to the rate, or from the outer to the inner area, with contribution $-k$:

$$k_n = \begin{cases} k, & \text{if } \bar{S}_T(t) \subset \{\bar{x}_p(t), \bar{v}_p(t) \mid p \text{ from inner to outer}\} \\ -k, & \text{if } \bar{S}_T(t) \subset \{\bar{x}_p(t), \bar{v}_p(t) \mid p \text{ from outer to inner}\}. \end{cases} \quad (13)$$

The value of k equals a contribution of one particle to the concentration at the transmitter location or, in other words, it is the constant difference in the particle concentration $\hat{c}_T(t)$ from consecutive time instants t_n, t_{n-1} :

$$k = \hat{c}_T(t_n) - \hat{c}_T(t_{n-1}). \quad (14)$$

The **nonuniform sampler** block samples at time instants t_n , which are functions of the transmitter kinetic state $\bar{S}_T(t)$. If, at time instant t_n , there is an event in the kinetic state $\bar{S}_T(t_n)$ concerning a particle changing its space area, the nonuniform sampler block produces a Dirac impulse at t_n , with amplitude equal to the current value of k_n , which is the output from the decision block:

$$k_n \delta(t - t_n) \text{ if } \bar{S}_T(t_n) \in \{\bar{x}_p(t_n), \bar{v}_p(t_n) \mid p \text{ changes space area}\}. \quad (15)$$

The **divisor** block divides the output of the sampler by the time interval between the previous sample at t_{n-1} and the current sample, which is at t_n . As a consequence, the output of the divisor block for the time interval $t_{n-1} < t < t_{n+1}$, which corresponds to the particle concentration rate $\hat{r}_T(t)$ affected by noise, is

$$\hat{r}_T(t) = \frac{k_n \delta(t - t_n)}{t_n - t_{n-1}} \text{ for } t_{n-1} < t < t_{n+1}. \quad (16)$$

For a time interval spanning from $t = 0$ to $t \rightarrow \infty$, the result is the expression introduced in (8).

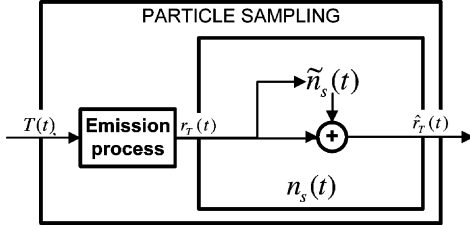


Fig. 7. Block scheme of the particle sampling noise stochastic model.

Since it is not possible to always have the knowledge of the kinetic state of the system $S_T(t)$ due to the huge amount of information and to the randomness in the particle motion, we cannot analytically compute the value of $\hat{r}_T(t)$ as function of $r_T(t)$ from the physical model of the particle sampling noise. Using the physical model provided here, we can only simulate the behavior of the particle sampling noise $n_s(t)$.

B. The Stochastic Model

The particle sampling noise can also have another formulation, through statistical parameters, which is suitable when theoretical studies require an analytical expression of the noise. For this, the particle sampling noise $n_s(t)$ is generated by a random process $\tilde{n}_s(t)$, whose contribution corresponds to the difference between the particle concentration rate $\hat{r}_T(t)$ affected by noise and the expected particle concentration rate $\langle \hat{r}_T(t) \rangle$, where $\langle \cdot \rangle$ denotes the ensemble average operator

$$\tilde{n}_s(t) = \hat{r}_T(t) - \langle \hat{r}_T(t) \rangle. \quad (17)$$

The expected particle concentration rate $\langle \hat{r}_T(t) \rangle$ corresponds to the time-continuous particle concentration rate that we would expect in the absence of the particle sampling noise:

$$\langle \hat{r}_T(t) \rangle = r_T(t). \quad (18)$$

In other words, $\tilde{n}_s(t)$ is an unwanted perturbation on the particle concentration rate around its expected value $r_T(t)$ due to the particle sampling noise. In Fig. 7, we show the main block scheme of “PARTICLE SAMPLING” when the stochastic model is applied for the particle sampling noise. The random process $\tilde{n}_s(t)$, as it is proved in the following, depends on the value of the particle concentration rate $r_T(t)$, output from the Emission Process block which receives the signal to be transmitted $T(t)$ as input. The sum of the random process $\tilde{n}_s(t)$ and the particle concentration rate $r_T(t)$ is the particle concentration rate affected by the particle sampling noise, namely, $\hat{r}_T(t)$.

In order to properly model the random process $\tilde{n}_s(t)$, we consider the following assumptions:

- The outer particle concentration at the transmitter $\hat{c}_T(t)$ increments/decrements its value whenever a single event concerning a particle changing its space area occurs.
- The probability of having two simultaneous events concerning particles changing their space area is zero. In other words, it is unlikely to have two particles crossing the spherical boundary of the transmitter at the same exact time instant. With reference to the physical model of the particle

sampling noise from Section III-A, this assumption translates into the statement: the probability of having two samples from the nonhomogeneous sampler at the same time instant is zero. In the equation, it becomes

$$\Pr[t_n - t_{n-1} = 0] = 0. \quad (19)$$

This assumption is justified by the independency of the Brownian components in the movement of different particles in the space. This assumption directly translates into the property of orderliness for the outer particle concentration $c_T(t)$ increments/decrements. The property of orderliness states that the probability that the difference between outer particle concentrations Δ time apart from each other is higher than the contribution k from a single particle, tends to zero as Δ tends to zero:

$$\lim_{\Delta \rightarrow 0} \Pr[|c_T(t + \Delta) - c_T(t)| > k] = 0 \quad (20)$$

where k is defined through (14).

- An event concerning a particle changing its space area (passing through an emission gap) occurring after time t is independent of any event of the same kind occurring before time t . This assumption is justified by the property of the Wiener process underlying the particle Brownian motion of having independent increments. As stated in Section III, particles are subject only to the contribution of the Brownian motion when they are located inside the inner area or the outer area. An event concerning a particle passing through an emission gap takes place whenever a particle, due to the Brownian motion, reaches the location of an emission gap: If there is a nonzero particle concentration rate in the outer area, the particle traverses the emission gap with net velocity $\bar{v}_p(t)$, given by (12). In other words, given a particle concentration rate in the outer area, which controls the average rate of occurrence of an event of this kind, the statistics of the event is solely dependent on the Brownian motion of the particles. As a consequence, the distribution of the time interval between an event at time $t - \Delta t$ and another event at time t is independent from the distribution of the time interval between an event at time t and an event at time $t + \Delta t$. The two distributions have the same expression from (11):

$$\begin{aligned} \Pr(b_x(t) - b_x(t - \Delta t) = x) &= \frac{1}{\sqrt{2\pi D \Delta t}} e^{-\frac{x^2}{2D\Delta t}} \\ &= \Pr(b_x(t + \Delta t) - b_x(t) = x) \end{aligned} \quad (21)$$

where $b_x(t)$ is the motion component along the \hat{i} versor at time t , D is the diffusion coefficient and Δt is positive. Equation (21) is valid also for the motion components $b_y(t)$ and $b_z(t)$ along the versors \hat{j} and \hat{k} , respectively. This implies that a particle motion from time t is independent from any motion of the particle occurred before time t . Being all the particles independent among each other, events concerning a change in the particle space area show the same independence. As a consequence, the events concerning particles changing their space area have the property of memorylessness.

- The occurrence rate of events concerning particles changing their space area is proportional to the flux of the particles between the inner area and the outer area.

The flux of the particles is proportional to the expected particle concentration rate at the transmitter location $r_T(t)$.

Under these assumptions [26], the resulting outer particle concentration at the transmitter $\hat{c}_T(t)$ is a double nonhomogeneous Poisson counting process, whose rate of occurrence corresponds to the expected particle concentration rate $r_T(t)$. The distribution of the outer particle concentration $\hat{c}_T(t)$ corresponds to a Poisson counting process with rate of occurrence $r_T(t)$ whenever the particle concentration rate $r_T(t)$ is positive. Whenever the particle concentration rate $r_T(t)$ is negative, $\hat{c}_T(t)$ is the negative of a Poisson counting process with rate of occurrence $-r_T(t)$:

$$\hat{c}_T(t) \sim \begin{cases} \text{Poiss}(r_T(t)) & r_T(t) > 0 \\ -\text{Poiss}(-r_T(t)) & r_T(t) < 0 \end{cases} \quad (22)$$

When the emission process is subject to the particle sampling noise, the particle concentration rate at the transmitter location $\hat{r}_T(t_n)$ corresponds to the first finite time difference of the particle concentration $\hat{c}_T(t)$, which is step-wise and, therefore, not derivable:

$$\hat{r}_T(t_n) = \frac{\hat{c}_T(t_n) - \hat{c}_T(t_{n-1})}{t_n - t_{n-1}}. \quad (23)$$

Since the particle concentration $\hat{c}_T(t)$ is a double nonhomogeneous Poisson counting process, the particle concentration rate at the transmitter location $\hat{r}_T(t)$ is the first finite time difference of a double nonhomogeneous Poisson counting process, whose average value $\langle \hat{r}_T(t) \rangle$, where $\langle \cdot \rangle$ denotes the ensemble average operator, has the same value as the rate of occurrence of the originating double Poisson counting process:

$$\langle \hat{r}_T(t) \rangle = r_T(t) \quad (24)$$

and whose autocorrelation is the expected squared particle concentration rate $r_T^2(t)$ added to the expected particle concentration rate $r_T(t)$ itself only for correlation lag l equal to 0:

$$\langle \hat{r}_T(t) \cdot \hat{r}_T(t+l) \rangle = r_T^2(t) + r_T(t)\delta(l) \quad (25)$$

where $\delta(l)$ is a Dirac delta. Given (17) and (18), the random process $\tilde{n}_s(t)$ has zero average value and its autocorrelation $R_s(t, l)$ is equal to the expected particle concentration rate $r_T(t)$ for correlation lag l equal to 0:

$$R_s(t, l) = \langle \tilde{n}_s(t) \cdot \tilde{n}_s(t+l) \rangle = r_T(t)\delta(l). \quad (26)$$

Therefore, the random process $\tilde{n}_s(t)$ is white [26], and its mean squared value is the expected particle concentration rate $r_T(t)$:

$$\langle \tilde{n}_s^2(t) \rangle = \langle \tilde{n}_s(t) \cdot \tilde{n}_s(t+l) \rangle|_{l=0} = r_T(t). \quad (27)$$

Taking into account (6), then the RMS of the perturbation RMS($\tilde{n}_s(t)$) on the expected particle concentration rate $r_T(t)$ is equal to the square root of the expected particle concentration rate $r_T(t)$:

$$\text{RMS}(\tilde{n}_s(t)) = \sqrt{r_T(t)}. \quad (28)$$

According to [17], the relation between the input signal $T(t)$ and the particle concentration rate $r_T(t)$ is expressed in the frequency (f) domain as

$$\tilde{r}_T(f) = \tilde{A}(f)\tilde{T}(f) \quad (29)$$

where $\tilde{T}(f)$ and $\tilde{r}_T(f)$ are the Fourier transforms [27] of the system input signal $T(t)$ and the particle concentration rate $r_T(t)$ at the transmitter location, respectively. $\tilde{A}(f)$ is the transfer function Fourier transform [27] (TFFT) of the transmitter module. The same relation in the time (t) domain becomes

$$r_T(t) = a(t) * T(t) \quad (30)$$

where $*$ denotes the convolution operator [27], $a(t)$ is the impulse response of the transmitter module and $T(t)$ is the input signal. The formula for the RMS of the perturbation RMS($\tilde{n}_s(t)$) on the signal $\hat{r}_T(t)$ becomes

$$\text{RMS}(\tilde{n}_s(t)) = \sqrt{a(t) * T(t)}. \quad (31)$$

IV. THE PARTICLE COUNTING NOISE

A. The Physical Model

The particle counting noise affects the physical end-to-end model from [17] at the signal propagation. When the particle concentration rate $\hat{r}_T(t)$ is being modulated at the transmitter location ($x = 0; y = 0; z = 0$), the signal propagates until reaching the receiver location ($x_R; y_R; z_R$), where the particle concentration value $c(x_R, y_R, z_R, t)$ is measured through the quantity $c_R(t)$. The propagation of the signal is achieved by means of the particle diffusion process, sketched in Fig. 8, which is based on the following assumptions:

- The linear size of the transmitter (radius of the spherical boundary) is considered negligible with respect to the distance between the transmitter and the receiver. Therefore, the *transmitter* is approximated as a *point-wise* concentration rate source at the location ($x = 0; y = 0; z = 0$).
- Particles are propagating from the transmitter location ($x = 0; y = 0; z = 0$) to the receiver location ($x_R; y_R; z_R$) solely by means of the laws of free diffusion in a fluidic medium.
- The measure of the particle concentration takes place inside the *receptor space*. The receptor space has a *spherical shape* of radius ρ .
- The particle concentration $c(x, y, z, t)$ is considered homogeneous inside the receptor space and equal to the particle concentration value at the receiver location, namely, $c(x_R, y_R, z_R, t)$.

The model of the particle diffusion process provided in [17] does not take into account the discrete nature of the particles and the randomness of their movements when the concentration $c(x_R, y_R, z_R, t)$ inside the receptor space is measured. Therefore, the measured particle concentration $c_R(t)$ is considered equal to the true particle concentration at the receiver location $c(x_R, y_R, z_R, t)$:

$$c_R(t) = c(x_R, y_R, z_R, t). \quad (32)$$

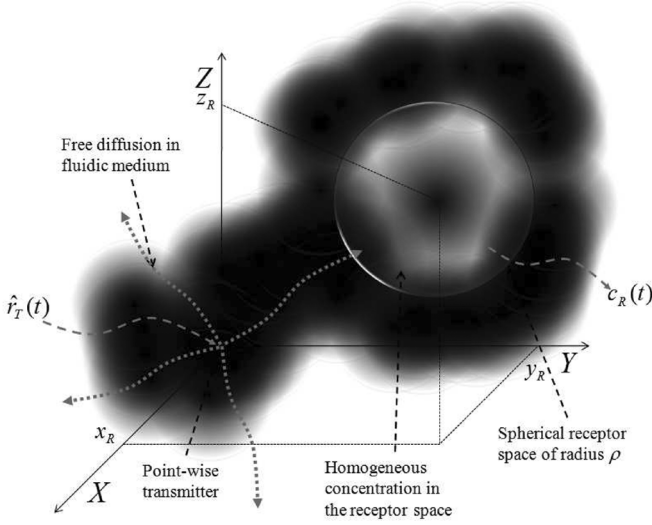


Fig. 8. Graphical sketch of the diffusion process.

In the present analysis, we introduce the following assumptions:

- The receptor space contains a *discrete number of particles*.
- Particles may enter/leave the receptor space due to the diffusion process, even when the concentration $c(x_R, y_R, z_R, t)$ at the receiver location is maintained at a constant value.

As a result, the measured particle concentration $\hat{c}_R(t)$ suffers from two effects. The first effect is given by the quantization of the concentration measure due to a discrete number of particles inside the receptor space. The second effect is given by fluctuations in the concentration measure due to single events of particles entering/leaving the receptor space. The overall process that takes the particle concentration rate $\hat{r}_T(t)$ as input and returns $\hat{c}_R(t)$ as output is called “PARTICLE COUNTING” and it is graphically sketched in Fig. 9. The “PARTICLE COUNTING” is composed of the Diffusion Process block and the particle counting noise block $n_c(t)$, as shown in Fig. 2. During the “PARTICLE COUNTING” particles present inside the receptor space at time instant t are counted, and their number $\hat{N}_p(t)$ is divided by the size of the receptor space $(4/3)\pi\rho^3$:

$$\hat{c}_R(t) = \frac{\hat{N}_p(t)}{(4/3)\pi\rho^3}, \quad \hat{N}_p(t) \in \mathbb{N} \quad (33)$$

where $\hat{N}_p(t)$ is a discrete integer number.

The “PARTICLE COUNTING” physical model is represented through the block scheme shown in Fig. 10. The particle concentration rate $\hat{r}_T(t)$ is the input of the Diffusion Process block, whose output is the true particle concentration $c_R(t)$. The physical model of the particle counting noise $n_c(t)$ takes as input the true particle concentration $c_R(t)$ that the diffusion process would produce in output in the absence of noise. The particle counting noise $n_c(t)$ is composed of two branches, as shown in Fig. 10. The upper branch has a decision block and a nonuniform sampler, which have as input the receiver kinetic state $\bar{S}_R(t)$, while the lower branch has a multiplier and rounder block and it takes as input the true particle concentration $c_R(t)$. The two branches are then added and the result is followed by

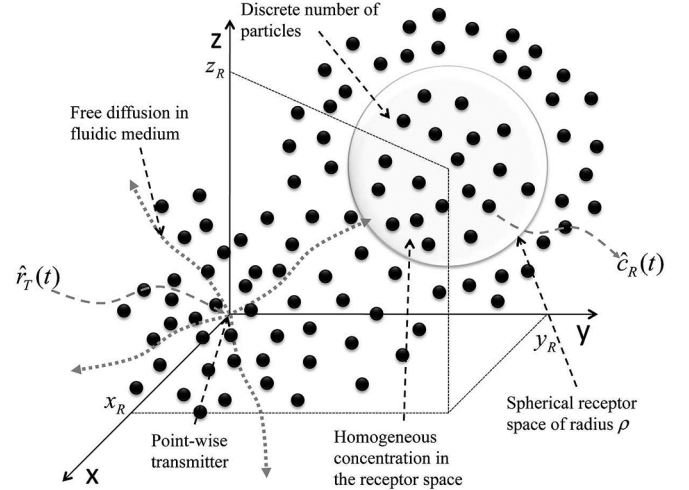


Fig. 9. Graphical sketch of the “PARTICLE COUNTING”: diffusion process and particle counting noise contribution.

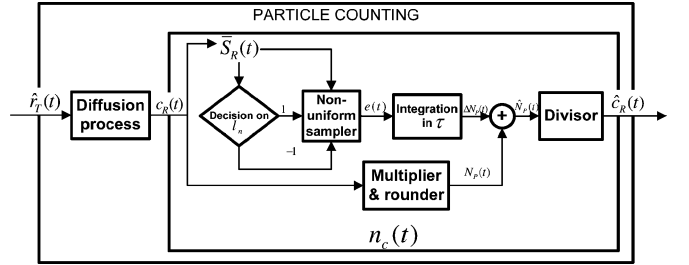


Fig. 10. Block scheme of the particle counting noise physical model.

a divisor. The output of the particle counting noise $n_c(t)$ is the particle concentration affected by noise, namely, $\hat{c}_R(t)$.

The **receiver kinetic state** $\bar{S}_R(t)$, as shown in Fig. 11, is a set composed by the location $\bar{x}_p(t)$ of each particle p at time t present in the surrounding of the receptor space:

$$\bar{S}_R(t) = \{\bar{x}_p(t) \mid p = 1, \dots, P(t)\} \quad (34)$$

where $P(t)$ is the number of particles in the system and varies as a function of the time t . In order to realistically simulate the receiver kinetic state $\bar{S}_R(t)$, we consider the Brownian motion contribution at every time instant t . The expression of the particle location $\bar{x}_p(t)$ is written as follows:

$$\bar{x}_p(t) = b_x(t)\hat{i} + b_y(t)\hat{j} + b_z(t)\hat{k} \quad (35)$$

where the Brownian motion velocity components, namely, $b_x(t)$, $b_y(t)$ and $b_z(t)$, are random variables with normal distribution, zero mean value and variance equal to $2D\delta t$, according to the expression of the Wiener process [26]:

$$b_x(t), b_y(t), b_z(t) \sim \mathcal{N}(0, 2D\delta t) \quad (36)$$

along the versors of the Cartesian axes, namely, \hat{i} , \hat{j} , and \hat{k} . D is the diffusion coefficient and δt is the simulation time step and it depends on how the receiver kinetic state is sampled during the physical model simulation. The smaller is the time step δt ,

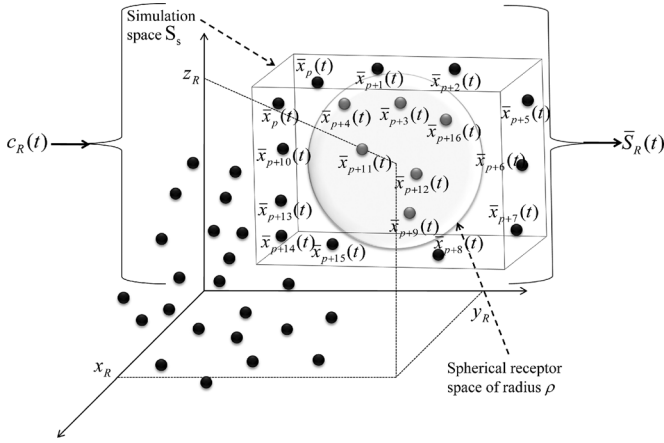


Fig. 11. Graphical sketch of the receiver kinetic state $\bar{S}_R(t)$ at time t . $\bar{S}_R(t)$ depends on the particle concentration $c_R(t)$ in input through the expressions in (34) and (35).

the closer is the simulation to the real physical phenomenon of particle diffusion. The particle number $P(t)$ is proportional to the particle concentration $c_R(t)$ multiplied by the size $\text{size}(\mathbf{S}_s)$ of the simulation space \mathbf{S}_s , shown in Fig. 11, which includes the receptor space

$$P(t) = c_R(t)\text{size}(\mathbf{S}_s). \quad (37)$$

The **decision** block assigns the value of l_n according to the receiver kinetic state $\bar{S}_R(t)$. l_n can assume either value 1 or -1 depending whether the kinetic state $\bar{S}_R(t)$ has an event concerning a particle that is entering or leaving the receptor space, respectively:

$$l_n = \begin{cases} 1 & \text{if } \bar{S}_R(t) \subset \{\bar{x}_p(t) \mid p \text{ enters the receptor space}\} \\ -1 & \text{if } \bar{S}_R(t) \subset \{\bar{x}_p(t) \mid p \text{ leaves the receptor space}\}. \end{cases} \quad (38)$$

The **nonuniform sampler** block samples at time instants t_n , which are functions of the receiver kinetic state $\bar{S}_R(t)$. If, at time instant t_n , there is an event in the kinetic state $\bar{S}_R(t_n)$ concerning a particle entering/leaving the receptor space, the nonuniform sampler block produces a Dirac impulse at t_n , with amplitude equal to the current value of l_n , in the output $e(t)$ from the decision block:

$$e(t) = l_n \delta(t - t_n) \text{if } \bar{S}_R(t_n) \subset \{\bar{x}_p(t_n) \mid p \text{ ent./leav.rec.space}\}. \quad (39)$$

The **integration** block integrates the output from the nonuniform sampler for a time interval equal to τ in the past up to time t , namely, $[t - \tau, t]$:

$$\Delta N_p(t) = \int_{t-\tau}^t e(t') dt'. \quad (40)$$

τ corresponds to the time interval in which we expect a quasi-constant particle concentration and its effect on the particle counting noise is further discussed in Section IV-B. The result of the integration block is the perturbation $\Delta N_p(t)$ at time t in the number of particles inside the receptor space.

The **multiplier and rounder** block rounds the particle concentration $c_R(t)$ multiplied by the size of the receptor space $(4/3)\pi\rho^3$. The output of this block corresponds to the expected number of particles $N_p(t)$ contained in the receptor space at time instant t :

$$N_p(t) = \text{round} \left[c_R(t) \left(\frac{4}{3}\pi\rho^3 \right) \right]. \quad (41)$$

The **divisor** block divides the sum of the output coming from the two branches, namely, $\Delta N_p(t)$ and $N_p(t)$, by the size of the receptor space $(4/3)\pi\rho^3$. As a consequence, the output of the divisor block corresponds to the particle concentration $\hat{c}_R(t)$ at the receiver affected by noise:

$$\hat{c}_R(t) = \frac{N_p(t) + \Delta N_p(t)}{\frac{4}{3}\pi\rho^3} = \frac{\hat{N}_p(t)}{\frac{4}{3}\pi\rho^3}. \quad (42)$$

Since it is not possible to always have knowledge of the kinetic state of the system $\bar{S}_R(t)$ due to the huge amount of information and to the randomness in the particle motion, we cannot analytically compute the value of $\hat{c}_R(t)$ as function of $c_R(t)$ from the physical model of the particle counting noise. Using the physical model provided here, we can only simulate numerically the behavior of the particle counting noise $n_c(t)$.

B. The Stochastic Model

The particle counting noise, similarly to the particle sampling noise, can also have another formulation, through statistical parameters, which is suitable when theoretical studies require an analytical expression of the noise. Statistical parameters for the particle counting noise, such as the RMS value, are provided in [21] without the definition of a complete stochastic model in terms of random processes. The derivation of these statistical parameters in [21] stems from a formulation of the particle counting noise in terms of macroscopic thermodynamic fluctuations in the system, without accounting for a particle-by-particle analysis. In this paper, we detail the knowledge of the particle counting noise by providing a stochastic model of the noise source. This model is obtained by stemming from the physical model outlined in Section IV-A, where the system is modeled in a particle-by-particle fashion. As will be proved in the following, the statistical parameters computed through the stochastic model provided here are in agreement with those from [21].

The particle counting noise $n_c(t)$ is generated by a random process $\tilde{n}_c(t)$, whose contribution corresponds to the difference between the measured particle concentration $\hat{c}_R(t)$ and the expected particle concentration $\langle \hat{c}_R(t) \rangle$, where $\langle \cdot \rangle$ denotes the ensemble average operator:

$$\tilde{n}_c(t) = \hat{c}_R(t) - \langle \hat{c}_R(t) \rangle. \quad (43)$$

The expected particle concentration $\langle \hat{c}_R(t) \rangle$ corresponds to the true particle concentration $c_R(t)$ that we would measure at the receiver in the absence of the particle counting noise:

$$\langle \hat{c}_R(t) \rangle = c_R(t). \quad (44)$$

In other words, $\tilde{n}_c(t)$ is an unwanted perturbation on the particle concentration measured at the receiver location around its expected value $c_R(t)$ due to the particle counting noise. In

Fig. 12 we show the main block scheme of the ‘‘PARTICLE COUNTING’’ when the stochastic model is applied for the particle counting noise. The random process $\tilde{n}_c(t)$, as it is proved in the following, depends on the value of the particle concentration at the receiver $c_R(t)$, output from the diffusion process, which receives the transmitted particle concentration rate $r_T(t)$ as input. The sum of the random process $\tilde{n}_c(t)$ and the true particle concentration at the receiver $c_R(t)$ is the particle concentration affected by the particle counting noise, namely, $\hat{c}_R(t)$. In order to properly model the random process $n_c(t)$ we consider the following assumptions:

- The actual number of particles $\hat{N}_p(t)$ inside the receptor space at time t is a random process whose average value is the true particle concentration at the receiver multiplied by the size of the receptor space:

$$\langle \hat{N}_p(t) \rangle = c_R(t) \frac{4}{3} \pi \rho^3. \quad (45)$$

- It is unlikely to have two particles occupying the same location in space at the same time instant t . In other words, the probability of having a distance equal to zero between two particles at the time instant t is zero:

$$\Pr[|\bar{x}_p(t) - \bar{x}_q(t)| = 0] = 0 \quad p \neq q, p, q \in [1, \dots, P(t)] \quad (46)$$

where $P(t)$ is given by (37), $\|\cdot\|$ is the Euclidian distance operator and p and q are two particles present in the simulation space \mathbf{S}_s defined in Section IV-A. This assumption is justified by the independence of the Brownian components in the movement of different particles in the space. This assumption directly translates into the property of orderliness for the counting process of the number of particles $\hat{n}_p(t, \bar{x}(t))$ at a location $\bar{x}(t)$ in the space

$$\lim_{\bar{\Delta} \rightarrow 0} \Pr[|\hat{n}_p(t, \bar{x}(t) + \bar{\Delta}) - \hat{n}_p(t, \bar{x}(t))| > 1] \rightarrow 0 \quad (47)$$

where $\bar{\Delta}$ is a movement in the three directions of the space from $\bar{x}(t)$ to $\bar{x}(t) + \bar{\Delta}$.

- An event concerning a particle which occupies a location in space $\bar{x}(t)$ is independent of any event of the same kind occurring at another space location $\bar{x}(t) + \bar{\Delta}$. This assumption is justified by the property of the Wiener process underlying the particle Brownian motion of having independent realizations. In other words, the distribution of the distance between the location of a particle in $\bar{x}(t)$ and another particle in $\bar{x}(t) + \bar{\Delta}_1$ is independent from the distribution of the distance between the same particle at $\bar{x}(t)$ and another particle present at location $\bar{x}(t) + \bar{\Delta}_2$, where $\bar{\Delta}_1 \neq \bar{\Delta}_2$. The two distributions have the same expression from (36):

$$\Pr(\|\bar{\Delta}_1\| = x) = \frac{1}{\sqrt{2\pi D \Delta t}} e^{-\frac{x^2}{2D \Delta t}} = \Pr(\|\bar{\Delta}_2\| = x). \quad (48)$$

This implies that the location of a particle is independent from the location of any other particle. As a consequence, the events concerning the location of particles in the space have the property of *memorylessness*.

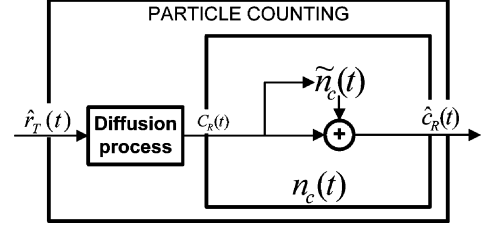


Fig. 12. Block scheme of the particle counting noise stochastic model.

- The occurrence rate of particle location in the space is proportional to the particle concentration at the receiver location $c(x_R, y_R, z_R, t)$, equal to the expected true particle concentration $c_R(t)$.

Under these assumptions, the resulting actual number of particles $\hat{N}_p(t)$ inside the receptor space is a volume nonhomogeneous Poisson counting process, whose rate of occurrence corresponds to the expected particle concentration $c_R(t)$:

$$\hat{N}_p(t) \sim \text{Poiss}(c_R(t)). \quad (49)$$

According to the Poisson process [26] in (49), the expected number of particles $\langle \hat{N}_p(t) \rangle$ contained in the receptor space can be computed by multiplying the volume Poisson process rate, which is the concentration $c_R(t)$, by the size of the receptor space $(4/3)\pi\rho^3$ and it is in agreement with the assumption made in (45). The variance in the number of particles contained in the receptor space has the same value as $\langle \hat{N}_p(t) \rangle$ [26]:

$$\langle (\hat{N}_p(t) - \langle \hat{N}_p(t) \rangle)^2 \rangle = c_R(t) \frac{4}{3} \pi \rho^3. \quad (50)$$

The actual measured particle concentration $\hat{c}_R(t)$ corresponds to the actual number of particles $\hat{N}_p(t)$ divided by the size of the receptor space

$$\hat{c}_R(t) = \frac{\hat{N}_p(t)}{(4/3)\pi\rho^3}. \quad (51)$$

Therefore, the average $\langle \hat{c}_R(t) \rangle$ of the actual measured particle concentration is equal to the expected particle concentration $c_R(t)$:

$$\langle \hat{c}_R(t) \rangle = c_R(t). \quad (52)$$

The variance of the actual measured particle concentration is equal to the expected particle concentration $c_R(t)$ divided by the size of the receptor space:

$$\langle (\hat{c}_R(t) - \langle \hat{c}_R(t) \rangle)^2 \rangle = \frac{\langle (\hat{N}_p(t) - \langle \hat{N}_p(t) \rangle)^2 \rangle}{(4/3)\pi\rho^3} = \frac{c_R(t)}{(4/3)\pi\rho^3}. \quad (53)$$

Given (43), (44), and (6), the random process $\tilde{n}_c(t)$ has zero average value and the RMS of the perturbation $\tilde{n}_c(t)$ on the actual measured particle concentration $\hat{c}_R(t)$ is

$$\text{RMS}(\tilde{n}_c(t)) = \sqrt{\langle (\hat{c}_R(t) - \langle \hat{c}_R(t) \rangle)^2 \rangle} = \sqrt{\frac{c_R(t)}{(4/3)\pi\rho^3}}. \quad (54)$$

It is possible to reduce the value of $\text{RMS}(\tilde{n}_c(t))$ by averaging in time a number M of measures of the particle concentration $\hat{c}_R(t)$:

$$\hat{c}_R(t) = \frac{1}{M} \sum_{m=1}^M \hat{c}_R(t - t_m). \quad (55)$$

The best results in terms of noise are obtained when the M measures are statistically independent. For this, we assume independent measures when they are taken at time instants spaced by an interval τ_p , as defined in [20]. If we assume to have a quasi-constant expected concentration in a time interval τ (which means that the bandwidth of the signal $c_R(t)$ is less than $1/\tau$ [27]), the maximum value of M is equal to the time interval τ divided by τ_p :

$$M = \frac{\tau}{\tau_p}; \quad (56)$$

thus, reducing the RMS of the perturbation $\text{RMS}(\tilde{n}_c(t))$ by a factor \sqrt{M}

$$\text{RMS}(\tilde{n}_c(t)) = \sqrt{\frac{c_R(t)}{(4/3)\pi\rho^3 M}}. \quad (57)$$

The waiting time τ_p corresponds to the average time required for a particle to leave the reception space. τ_p is equal to the average distance to the spherical boundary, divided by the velocity of a particle v_p . The average distance corresponds to the receptor space radius ρ :

$$\tau_p = \frac{\rho}{v_p}. \quad (58)$$

The velocity v_p of a particle comes from the first Fick's law of diffusion [10], [11]. For this, the particle concentration flux $\bar{J}(\bar{x}, t)$ at time instant t and location \bar{x} , is equal to the spatial gradient (operator ∇) of the particle concentration $c(\bar{x}, t)$ multiplied by the diffusion coefficient D :

$$\bar{J}(\bar{x}, t) = -D\nabla c(\bar{x}, t). \quad (59)$$

When we have homogeneous concentration \bar{c} inside the receptor space and zero concentration outside the receptor space, $\nabla c(\bar{x}, t)$ is equal to the opposite $-\bar{c}$ of the concentration divided by the radius ρ of the receptor space. Further, the particle concentration flux $\bar{J}(\bar{x}, t)$ is equal, by definition, to the particle concentration \bar{c} multiplied by the particle velocity v_p . If we solve (59) for the particle velocity, we obtain

$$v_p = \frac{D}{\rho}. \quad (60)$$

The average time τ_p is therefore equal to the radius ρ squared and divided by the diffusion coefficient D

$$\tau_p = \frac{\rho^2}{D} \quad (61)$$

which is in agreement with the results from [20], [21]. The final expression for the RMS of the perturbation $\text{RMS}(\tilde{n}_c(t))$ becomes

$$\text{RMS}(\tilde{n}_c(t)) = \sqrt{\frac{c_R(t)}{(4/3)\pi D \rho \tau}} \quad (62)$$

where $c_R(t)$ is the expected measured particle concentration, D is the diffusion coefficient, ρ is the radius of the receptor space and τ is the time interval in which we expect a quasi-constant particle concentration. The validity of (62) is confirmed by the results from [21], where the authors reach the same expression for the RMS of the particle counting noise by applying a different approach, as explained above.

According to [17], the relation between the input particle concentration rate $\hat{r}_T(t)$ and the measured particle concentration $c_R(t)$ at the receiver location is expressed in the frequency (f) domain as

$$\tilde{c}_R(f) = \tilde{\mathbf{B}}(f)\tilde{\hat{r}}_T(f) \quad (63)$$

where $\tilde{\hat{r}}_T(f)$ and $\tilde{c}_R(f)$ are the Fourier transforms [27] of the particle concentration rate $\hat{r}_T(t)$ and the particle concentration $c_R(t)$, respectively. $\tilde{\mathbf{B}}(f)$ is the TFFT [27] of the propagation module. The same relation in the time (t) domain becomes

$$c_R(t) = b(t) * \hat{r}_T(t) \quad (64)$$

where $*$ denotes the convolution operator [27], $b(t)$ is the impulse response of the propagation module and $\hat{r}_T(t)$ is the input particle concentration rate. The formula for the RMS of the perturbation $\text{RMS}(\tilde{n}_c(t))$ on the signal $\hat{c}_R(t)$ becomes

$$\text{RMS}(\tilde{n}_c(t)) = \sqrt{\frac{b(t) * \hat{r}_T(t)}{(4/3)\pi D \rho \tau}} \quad (65)$$

where D is the diffusion coefficient, ρ is the radius of the spherical receptor space, and τ is the time in which we expect a quasi-constant particle concentration.

V. SIMULATIONS

In this section, we present a numerical analysis of the diffusion-based noise models. Sets of noise data realizations are generated through simulation of the physical model. These sets of noise data are then used to test the stochastic model ability to capture the behavior of the physical processes which generate the noise.

A. The Particle Sampling

The simulations of the physical model for the particle sampling noise are computed by applying to the scheme in Fig. 5 a sinusoidal signal in the particle concentration rate $r_T(t)$:

$$r_T(t) = A \sin(2\pi f_a t) \quad (66)$$

where f_a is the frequency of the sinusoid in hertz, A is the value of the maximum particle concentration rate in particles $\mu\text{m}^{-3}\text{s}^{-1}$, and t is the simulation time index in milliseconds.

The input of the physical model simulation is a sinusoidal particle concentration rate $r_T(t)$ with frequency f_a equal to

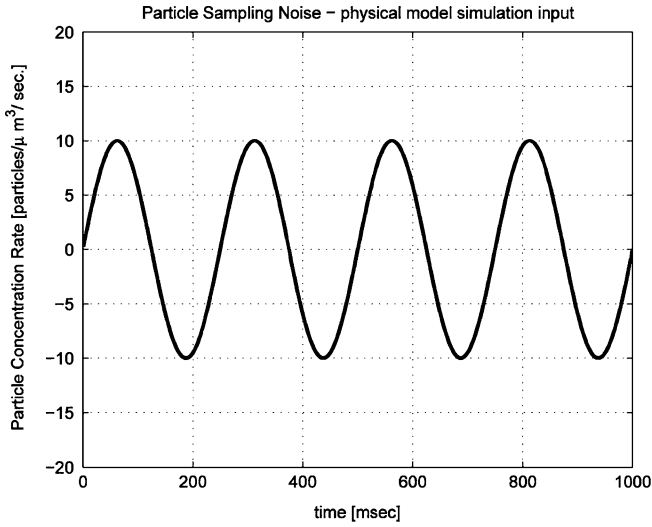


Fig. 13. The particle sampling noise physical model simulation input.

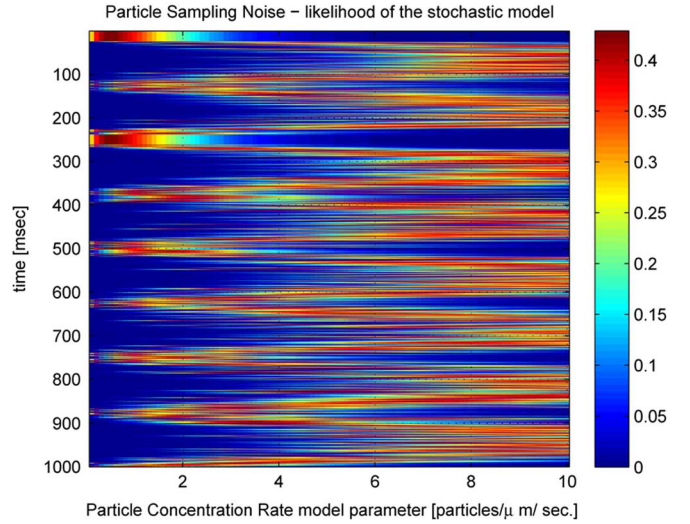


Fig. 15. The particle sampling stochastic model likelihood.

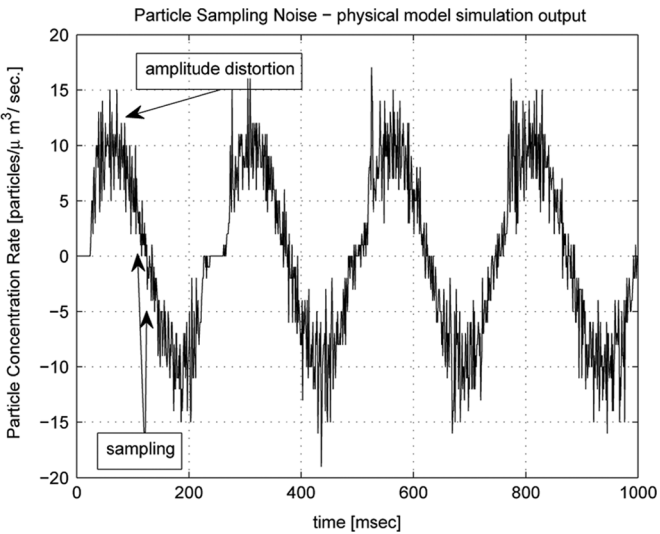


Fig. 14. The particle sampling noise physical model simulation output.

4 Hz and maximum particle concentration rate A of 10 particles $\mu\text{m}^{-3}\text{s}^{-1}$, as shown in Fig. 13. The radius of the transmitter spherical boundary is $\rho = 1 \mu\text{m}$. The simulation runs for 1 s by steps of $\delta t = 1 \text{ ms}$. The output noisy particle concentration rate $\hat{r}_T(t)$ of the physical model simulation is shown in Fig. 14.

During the simulation, particles are generated inside the transmitter spherical boundary at random locations whenever the particle concentration rate $r_T(t)$ is positive. Particle deletion is randomly performed inside the transmitter spherical boundary whenever $r_T(t)$ is negative. Through particle generation and particle deletion we control the number of particles in the system $P(t)$, which is a parameter of the transmitter kinetic state $\bar{S}_T(t)$ shown in (9). The Brownian motion of the particles is modeled according to (10) and having the diffusion coefficient $D \sim 10^{-6} \text{ cm}^2 \text{ s}^{-1}$ of calcium molecules diffusing in a biological environment (cellular cytoplasm, [28]). Samples contributing to the value of $\hat{r}_T(t)$ are generated by applying (13) and (15) to the transmitter kinetic state $\bar{S}_T(t)$. The final results in terms of particle concentration rate $\hat{r}_T(t)$ is achieved by applying (16).

The particle sampling noise has two different effects on the sinusoidal signal, namely, signal sampling and signal amplitude distortion. Signal sampling is given by the nonhomogeneous sampling of the particle concentration rate $r_T(t)$ in time, as shown in Fig. 14. In nonhomogeneous sampling, samples are separated by a nonconstant time interval. Since in the simulations we apply a constant time step δt , for each time steps the contributions of samples which occur within δt are added. The signal amplitude distortion is given by the constant contribution that each particle gives to the concentration at the transmitter location, (14), whenever a sample is generated by the nonhomogeneous sampling. Constant contributions in nonhomogeneous sampling cause sudden changes in the particle concentration rate value, which result in distortions of its amplitude.

The statistical likelihood test is applied in order to assess the stochastic model ability to capture the behavior of the physical processes which generate the noise. For this, we compute the likelihood, that is, the probability of the noisy data coming from the physical model simulation $\hat{r}_T(t)$ given the stochastic model of the particle sampling noise, as defined in Section III-B. In order to evaluate the reliability of the particle sampling stochastic model parameters in (25) and (27), the likelihood probability is evaluated for a range of different values for the parameter $r_T(t)$ of the Poisson processes in (22):

$$\begin{aligned} \text{likelihood}_{\text{Particle Sampling}} \\ = \Pr(\hat{r}_T(t) | \text{Part.Sampl.stor}_T(t)) \end{aligned} \quad (67)$$

where $r_T(t)$ ranges from 0.1 to 10 particles $\mu\text{m}^{-3} \text{ s}^{-1}$ for every time instant t . The results are shown in Fig. 15, where it is clearly visible that the highest likelihood value corresponds, for every time instant t , to the value of $r_T(t)$ from (66), thus confirming that the best particle concentration rate, parameter of the model, is actually the particle concentration rate in input to the physical model of the particle sampling noise.

This statistical likelihood test results shown in Fig. 15 are compared to the results obtained through the use of a Gaussian model in place of the particle sampling noise stochastic model. The Gaussian model, denoted by $\mathcal{N}(r_T(t), r_T(t))$ has the same

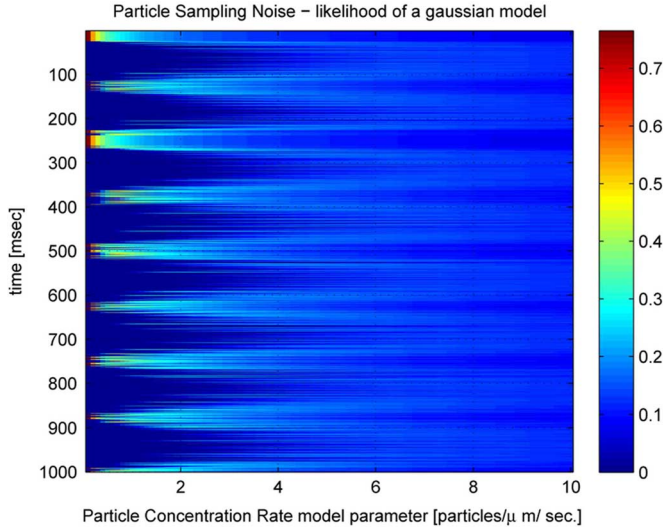


Fig. 16. The Gaussian model likelihood for the particle sampling noise.

expected value and the same variance as the particle sampling noise stochastic model. The likelihood formula is

$$\text{likelihood}_{\text{Gaussian}} = \Pr(\hat{r}_T(t) | \mathcal{N}(r_T(t), r_T(t))) \quad (68)$$

where $r_T(t)$ ranges from 0.1 to 10 particles $\mu\text{m}^{-3}\text{s}^{-1}$ for every time instant t . The results in terms of Gaussian model likelihood are shown in Fig. 16. When the Gaussian model is applied, the likelihood shows higher values than when using the particle sampling stochastic model, but only at specific time instants. On average, the likelihood values shown in Fig. 16 are much lower than the values in Fig. 15 and this proves that the particle sampling stochastic model performs better than the Gaussian model. This preliminary result confirms the validity of the particle sampling stochastic model presented in this paper.

B. The Particle Counting

The simulations of the physical model for the particle counting noise are computed by applying to the scheme in Fig. 10 a sinusoidal signal in the true particle concentration at the receiver $c_R(t)$:

$$c_R(t) = B \sin(2\pi f_b t) + B \quad (69)$$

where f_b is the frequency of the sinusoid in Hz, $2B$ is the maximum value of the expected particle concentration in particles μm^{-3} , and t is the simulation time index in milliseconds.

The input of the physical model simulation is a sinusoidal particle concentration $c_R(t)$ with frequency f_b equal to 4 Hz and maximum particle concentration $2B$ of 2000 particles μm^{-3} , as shown in Fig. 17. The radius of the spherical receptor space is $\rho = 1 \mu\text{m}$. The simulation runs for 1 s by steps of $\delta t = 1 \text{ ms}$. The output noisy particle concentration $\hat{c}_R(t)$ of the physical model simulation is shown in Fig. 18.

A number $P(t)$ of particles are deployed according to (37) for each time at random locations inside the simulation space \mathbf{S}_s , shown in Fig. 11, which includes the receptor space. The receptor kinetic state is maintained according to (34) and (35), where the Brownian motion of the particles is modeled according to (36). The diffusion coefficient $D \sim 10^6 \text{ cm}^2\text{s}^{-1}$

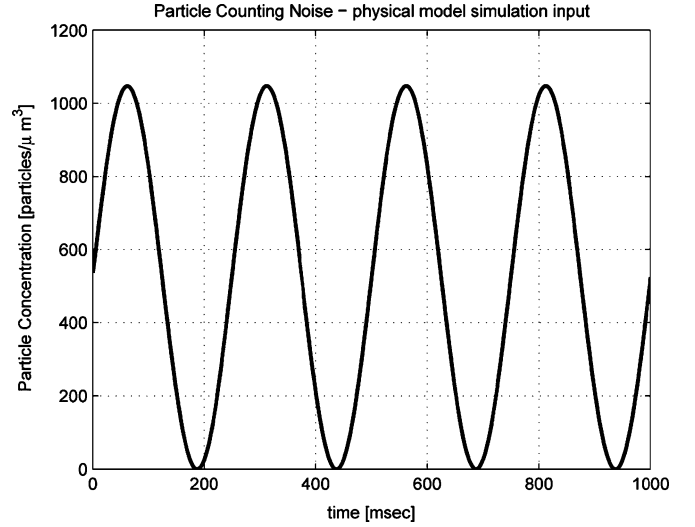


Fig. 17. The particle counting noise physical model simulation input.

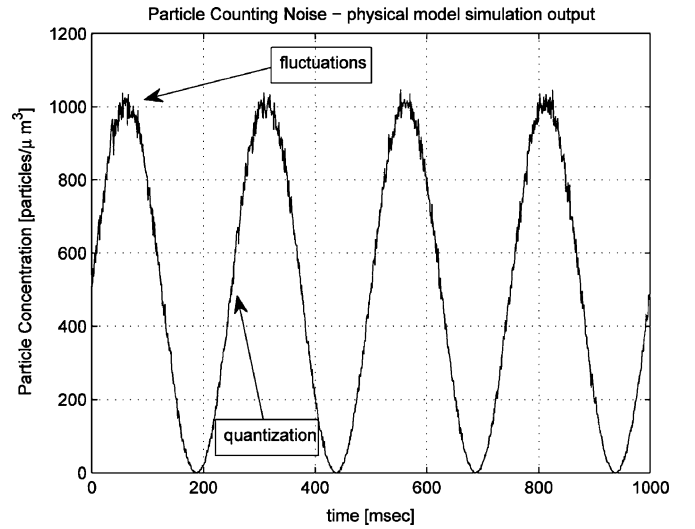


Fig. 18. The particle counting noise physical model simulation output.

corresponds to the D of calcium molecules diffusing in a biological environment (cellular cytoplasm, [28]). The upper branch of Fig. 10, which generates the contribution ΔN_p to the final result, is computed by applying (38) and (39) to the transmitter kinetic state $\bar{S}_T(t)$. Equation (40) is applied with a value $\tau = 1 \text{ ms}$, equal to a simulation step. The lower branch of Fig. 10 gives the second contribution to the final result and includes the computation of $N_p(t)$ through (41). The final results in terms of particle concentration $\hat{c}_R(t)$ is achieved by applying (42) to the sum of the outputs from the upper branch and the lower branch.

The particle counting noise is visible through two effects, as shown in Fig. 18. The first effect is given by the quantization of the concentration measure by a discrete number of particles inside the receptor space. The second effect is given by fluctuations in the concentration measure due to single events of particles entering/leaving the receptor space. The latter is more accentuated for high values of the particle concentration. This behavior is a confirmation of the fact that the RMS value of the particle counting noise is proportional to the square root of the

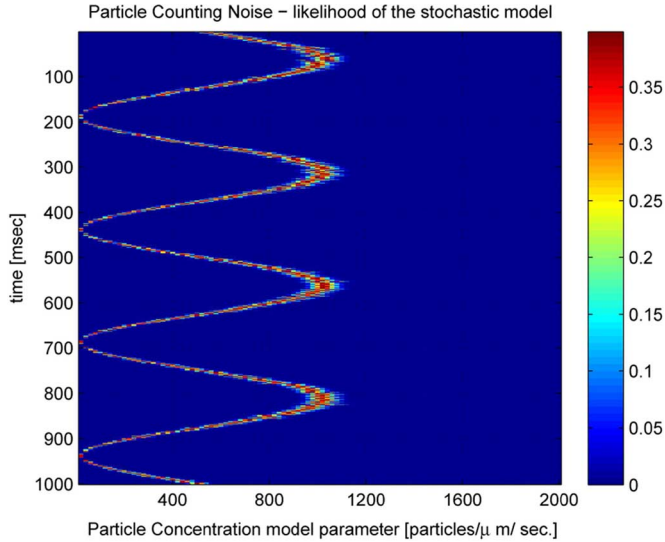


Fig. 19. The particle counting stochastic model likelihood.

true particle concentration $c_R(t)$, as shown in (54), (57), and (62).

The statistical likelihood test is applied in order to assess the stochastic model ability to capture the behavior of the physical processes which generate the noise. For this, we compute the likelihood, that is, the probability of the noisy data coming from the physical model simulation $\hat{c}_R(t)$ given the stochastic model of the particle counting noise, as defined in Section IV-B. In order to evaluate the reliability of the particle counting stochastic model parameters in (52) and (53), the likelihood probability is evaluated for a range of different values for the parameter $c_R(t)$ of the Poisson processes in (49):

$$\text{likelihood}_{\text{Particle Counting}} = \Pr(\hat{c}_R(t) | \text{Part.Count.stoc} c_R(t)) \quad (70)$$

where $c_R(t)$ ranges from 1 to 2000 particles μm^{-3} for every time instant t . The results are shown in Fig. 19, where it is clearly visible that the highest likelihood value corresponds, for every time instant t , to the value of $c_R(t)$ from (69), thus confirming that the best particle concentration model parameter is actually the particle concentration in input to the physical model of the particle counting noise.

This statistical likelihood test results shown in Fig. 19 are compared to the results obtained through the use of a Gaussian model in place of the particle counting noise stochastic model. The Gaussian model, denoted $\mathcal{N}(c_R(t), c_R(t)/(4/3\pi\rho^3))$ has the same expected value and the same variance as the particle sampling noise stochastic model. The likelihood formula is

$$\text{likelihood}_{\text{Gaussian}} = \Pr\left(\hat{c}_R(t) | \mathcal{N}\left(c_R(t), \frac{c_R(t)}{(4/3\pi\rho^3)}\right)\right) \quad (71)$$

where $c_R(t)$ ranges from 1 to 2000 particles μm^{-3} for every time instant t and $\rho = 1 \mu\text{m}$. The comparison between the Gaussian model likelihood and the particle counting stochastic model drives us to the same conclusions we had for the particle sampling noise. At specific time instants, the Gaussian model likelihood shows higher values than when using the particle

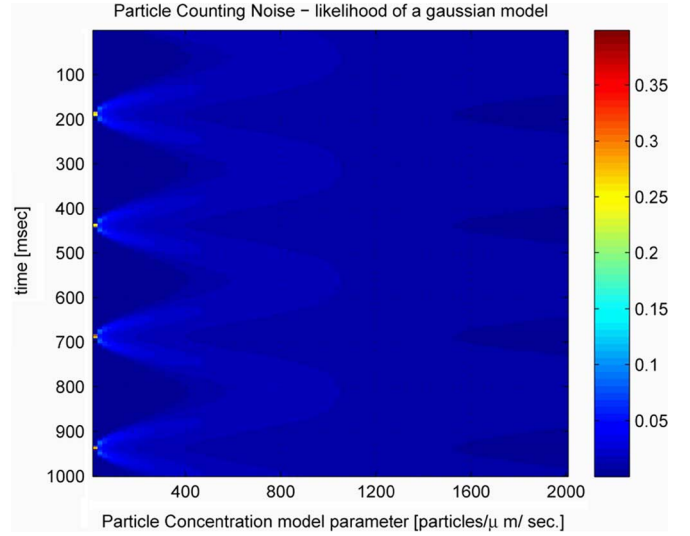


Fig. 20. The Gaussian model likelihood for the particle counting noise.

counting stochastic model but, on average, the likelihood values shown in Fig. 20 are much lower than the values in Fig. 19. This proves that the particle counting stochastic model performs better than the Gaussian model and it confirms the stochastic model ability to express the behavior of the physical processes underlying the particle counting noise.

VI. CONCLUSION

In this paper we analyze the most relevant diffusion-based noise sources affecting MC. To date, little effort has been made to model the diffusion-based noise sources from the communication engineering perspective, while contributions from the biochemistry literature provide descriptions of some underlying physical processes. However, these contributions tend to focus on the explanation of natural phenomena and do not provide suitable models for MC engineering. The objective of this work is the analysis of the noise sources in diffusion-based MC using tools from signal processing, statistics and communication engineering, with reference to the diffusion-based MC system introduced in [17].

The particle sampling noise and the particle counting noise are identified in this paper as the most relevant diffusion-based noise sources affecting the MC physical end-to-end model from [17]. The analysis of the noise sources results both in physical models and stochastic models. With the former we aim at the mathematical expression of the physical processes underlying the noise sources, while with the latter we model the noise source behaviors through the use of statistical parameters. For both the two noise sources, the results of the physical models are summarized through block schemes, which expand the end-to-end physical model from [17]. The stochastic models of both the two noise sources result in their characterization in terms of random processes and in the analytical expression of the RMS perturbation of the noise on the information signal.

Simulations are shown to evaluate the capability of the stochastic models to express the diffusion-based noise sources represented by means of the physical models.

The results coming from this work will be used to have a better insight into the end-to-end diffusion-based MC, especially in terms of capacity and throughput. We believe that this

paper provides a preliminary study on the noise affecting the end-to-end diffusion-based MC, and that further investigation on this topic is necessary.

ACKNOWLEDGMENT

The authors would like to thank J. M. Jornet, I. Llatser, and N. Garralda for their constructive criticism which helped to improve the quality of the paper, and the referees for their excellent and constructive feedback.

REFERENCES

- [1] I. F. Akyildiz, F. Brunetti, and C. Blazquez, "Nanonetworks: A new communication paradigm at molecular level," *Comput. Netw.*, vol. 52, no. 12, pp. 2260–2279, Aug. 2008.
- [2] L. Parcerisa and I. F. Akyildiz, "Molecular communication options for long range nanonetworks," *Comput. Netw.*, vol. 53, no. 16, pp. 2753–2766, Aug. 2009.
- [3] M. Moore, A. Enomoto, T. Nakano, R. Egashira, T. Suda, A. Kaya-suga, H. Kojima, H. Sakakibara, and K. Oiwa, "A design of a molecular communication system for nanomachines using molecular motors," in *Proc. 4th Annu. IEEE Int. Conf. Pervasive Comput. Commun. Workshops*, Mar. 2006, pp. 6–12.
- [4] M. Gregori and I. F. Akyildiz, "A new nanonetwork architecture using flagellated bacteria and catalytic nanomotors," *IEEE J. Sel. Areas Commun.*, vol. 28, no. 4, pp. 602–611, May 2010.
- [5] M. J. Berridge, "The AM and FM of calcium signalling," *Nature*, vol. 386, no. 6627, pp. 759–780, Apr. 1997.
- [6] W. H. Bossert and E. Wilson, "The analysis of olfactory communication among animals," *J. Theor. Biol.*, vol. 5, no. 3, pp. 443–469, Nov. 1963.
- [7] T. Nakano, T. Suda, M. Moore, R. Egashira, A. Enomoto, and K. Arima, "Molecular communication for nanomachines using intercellular calcium signaling," in *Proc. 5th IEEE Conf. Nanotechnol.*, Jul. 2005, vol. 2, pp. 478–481.
- [8] P. J. W. Roberts and D. R. Webster, "Turbulent diffusion," in *Environmental Fluid Mechanics-Theories and Application*, H. H. Shen, Ed. New York: Amer. Soc. Civil Eng., 2002.
- [9] I. Rubinstein, *Electro-Diffusion of Ions*, ser. SIAM Studies in Applied Mathematics. Philadelphia, PA: SIAM, 1990, vol. 11.
- [10] J. Philibert, "One and a half century of diffusion: Fick, Einstein, before and beyond," *Diffusion Fundam.*, vol. 4, pp. 6.1–6.19, 2006.
- [11] E. L. Cussler, "Diffusion," in *Mass Transfer in Fluid Systems*, 2nd ed. Cambridge, U.K.: Cambridge Univ. Press, 1997.
- [12] G. Alfano and D. Miorandi, "On information transmission among nanomachines," in *Proc. 1st Int. Conf. Nano-Netw. Workshops*, Sep. 2006, pp. 1–5.
- [13] S. Kadloor and R. Adve, "A framework to study the molecular communication system," in *Proc. 18th Int. Conf. Comput. Commun. Netw.*, Aug. 2009, pp. 1–6.
- [14] B. Atakan and O. B. Akan, "An information theoretical approach for molecular communication," in *Proc. 2nd Conf. Bio-Inspired Models Netw., Inf., Comput. Syst.*, Dec. 2007, pp. 33–40.
- [15] B. Atakan and O. B. Akan, "On molecular multiple-access, broadcast, and relay channels in nanonetworks," in *Proc. 3rd Int. Conf. Bio-Inspired Models Netw., Inf., Comput. Syst.*, Nov. 2008, pp. 16:1–16:8.
- [16] D. J. Spencer, S. K. Hampton, P. Park, J. P. Zurkus, and P. J. Thomas, "The diffusion-limited biochemical signal-relay channel," in *Proc. Adv. Neural Inf. Process. Syst.*, vol. 16, 2004, MIT Press.
- [17] M. Pierobon and I. F. Akyildiz, "A physical end-to-end model for molecular communication in nanonetworks," *IEEE J. Sel. Areas Commun.*, vol. 28, no. 4, pp. 602–611, May 2010.

- [18] M. J. Moore, T. Suda, and K. Oiwa, "Molecular communication: Modeling noise effects on information rate," *IEEE Trans. Nanobiosci.*, vol. 8, no. 2, pp. 169–180, Jun. 2009.
- [19] B. Atakan and O. B. Akan, "On channel capacity and error compensation in molecular communication," *Trans. Comput. Syst. Biol. X*, pp. 59–80, 2008.
- [20] H. Berg and E. Purcell, "Physics of chemoreception," *Biophys. J.*, vol. 20, no. 2, pp. 193–219, Nov. 1977.
- [21] W. Bialek and S. Setayeshgar, "Physical limits to biochemical signaling," in *Proc. Nat. Acad. Sci. USA*, Jul. 2005, vol. 102, no. 29, pp. 10 040–10 045.
- [22] K. Prank, F. Gabbiani, and G. Brabant, "Coding efficiency and information rates in transmembrane signaling," *Biosyst.*, vol. 55, no. 1–3, pp. 15–22, Feb. 2000.
- [23] J.-Q. Liu and T. Nakano, "An information theoretic model of molecular communication based on cellular signaling," in *Proc. 2nd Conf. Bio-Inspired Models Netw., Inf., Comput. Syst.*, Dec. 2007, pp. 316–321.
- [24] D. L. Nelson and M. M. Cox, *Lehninger Principles of Biochemistry*. San Francisco, CA: Freeman, 2005, ch. 12.2, pp. 425–429.
- [25] H. Nyquist, "Certain topics in telegraph transmission theory," *Proc. IEEE*, vol. 90, no. 2, pp. 280–305, Feb. 2002, Reprint as Classic Paper.
- [26] A. Papoulis and S. U. Pillai, *Probability, Random Variables and Stochastic Processes*, 4th ed. New York: McGraw-Hill, 2002.
- [27] B. Davies, *Integral Transforms and Their Applications*. New York: Springer, 2002.
- [28] B. S. Donahue and R. F. Abercrombie, "Free diffusion coefficient of ionic calcium in cytoplasm," *Cell Calcium*, vol. 8, no. 6, pp. 437–448, Dec. 1987.



Massimiliano Pierobon (S'09–M'09) received the M.S. degree from telecommunication engineering at the Politecnico di Milano, Italy, in 2005.

During 2006, he worked as a researcher in the R&D department of Siemens Carrier Networks, Milan, Italy. From January 2007 to July 2009, he was a graduate Research Assistant at the Politecnico di Milano. From November 2008 until July 2009, he was a visiting researcher at the BWN lab of the School of Electrical and Computer Engineering, Georgia Institute of Technology, Atlanta, where he joined as a Ph.D. student in August 2009. His research interests are in molecular communication for nanoscale networks.



Ian F. Akyildiz (M'86–SM'89–F'96) received the B.S., M.S., and Ph.D. degrees in computer engineering from the University of Erlangen-Nürnberg, Germany, in 1978, 1981, and 1984, respectively.

Currently, he is the Ken Byers Chair Professor with the School of Electrical and Computer Engineering, Georgia Institute of Technology (Georgia Tech), Atlanta, the Director of Broadband Wireless Networking Laboratory, and Chair of the Telecommunication Group at Georgia Tech. In June 2008, he became an honorary professor with the School of Electrical Engineering, Universitat Politècnica de Catalunya (UPC), Barcelona, Spain. He is also the Director of the newly founded N3Cat (NaNoNetworking Center in Catalunya). He has also been an Honorary Professor with University of Pretoria, South Africa, since March 2009. His research interests are in nanonetworks, cognitive radio networks, and wireless sensor networks.

Dr. Akyildiz is the Editor-in-Chief of the Elsevier journals *Computer Networks*, and the founding Editor-in-Chief of the *Ad Hoc Networks Journal*, the *Physical Communication Journal*, and the *Nano Communication Networks Journal*. He serves on the advisory boards of several research centers, journals, conferences, and publication companies. He has been an ACM Fellow since 1997. He received numerous awards from the IEEE and the ACM.